Developing high performance RF heating scenarios on the WEST tokamak

Marc Goniche, Clarisse Bourdelle, J.F. Artaud, Jean-Michel Bernard, Jérôme Bucalossi, Laurent Colas, Corinne Desgranges, Delpech Léna, P Devynck, V. Bobkov, et al.

HAL Id: cea-03520558

https://cea.hal.science/cea-03520558

Submitted on 11 Jan 2022

DEVELOPING HIGH PERFORMANCE RF HEATING SCENARIOS ON THE WEST TOKAMAK

M.GONICHE, C.BOURDELLE, J.F.ARTAUD, J.M.BERNARD, J.BUCALOSSI, L.COLAS, C.DESGRANGES, L.DELPECH, P.DEVYNCK, R.DUMONT, A.EKEDAHL, N.FEDORCZAK, J.GARCIA, C.GIL, C.GUILLEMAUT, J.GUNN, J.HILLAIRET, G.LOMBARD, P.MAGET, P.MANAS, D.MAZON, O.MEYER, J.MORALES, Ph.MOREAU, E.NARDON, R.NOUAILLETAS, V.OSTUNI, M.PERET, Y.PEYSSON, X. REGAL-MEZIN, G.URBANCZYK, D.VEZINET and the WEST Team*
CEA, IRFM, F-13108 Saint Paul-lez-Durance, France
marc.goniche@cea.fr

V.BOBKOV
Max-Planck Institut für plasmaphysik, Boltzmannstraße 2, 85748 Garching, Germany

J.GASPAR
Aix Marseille Univ, CNRS, IUSTI, Marseille, France

C.C.KLEPPER, C.LAU, E.H.MARTIN
Oak Ridge National Laboratory, Oak Ridge, Tennessee 37831-6169, USA

E.LERCHE
Laboratory for Plasma Physics, Royal Military Academy, 1000 Bruxelles, Belgium

S.SHIRAIWA·
Princeton Plasma Physics Laboratory, Princeton, USA

L.VERMARE
Ecole Polytechnique, LPP, CNRS UMR 7648, 91128 Palaiseau cedex. France

G.M.WALLACE
MIT Plasma Science and Fusion Center, Cambridge, MA 02139, USA

*http://west.cea.fr/WESTteam

Abstract

High power experiments, up to 9.2 MW with LHCD and ICRH, have been carried out in the full tungsten tokamak WEST. Quasi non inductive discharges have been achieved allowing to extend the plasma duration to 53s at medium density (n_e=3.7×10^{19}m^{-3}). Apart few pulses post-boronization, the plasma radiation is rather high (Prad/Ptot~50%) and is dominated by W. This fraction does not vary as the RF power is ramped up and, against expectations, it is quite similar in ICRH and/or LHCD heated plasmas. Hot L mode plasmas (T_e(0)>3keV) with a confinement time following the ITER L96 scaling are routinely obtained, confirming the weak aspect ratio dependence of this scaling law. Tungsten accumulation is generally not an operational issue on WEST. Nonetheless, 25% of the of the discharges are affected by a rapid collapse of the central electron temperature which occurs when a slight decrease of T_e leads to enhanced radiation causing flat or hollow current profiles. To this respect LHCD-only discharges are compared to ICRH and ICRH/LHCD discharges.

1. INTRODUCTION

WEST is a medium size (R=2.5m, a=0.45m) actively cooled full W tokamak aiming at power exhaust studies in long / steady-state pulses. WEST can operate in lower single null (USN), upper single null (USN) and double null configurations with an aspect ratio of 5-6. The lower divertor was partially made of ITER-like target in phase 1 (2017-2021), it will be fully made of ITER-like PFC in phase 2 starting summer 2021 [1,]. For this purpose two lower hybrid current drive (LHCD) launchers and three ion cyclotron resonance heating (ICRH) antennas, have been installed and commissioned. All antennas are actively-cooled and equipped by tungsten-coated guard limiters.
In the 2019 and 2020-21 campaigns, the LHCD and ICRH coupled powers have both reached ~5MW/1s separately (up to 5.3MW/4s for LHCD) and 8.8MW/0.5s when combining the two RF systems [2, 3]. Long pulse operation was

also carried out with LHCD (P_{LH}=3.0MW) extending the pulse length to 55 seconds .The experiments were performed at high magnetic field (B_t=3.6-3.7T) in a large range of plasma configurations: X-point plasmas (R~2.5m, a~0.45m, κ~1.3) in LSN and USN configuration, plasma current in the 0.3-0.7MA range (q_{95}~3-6), line-averaged electron density in the 2.5-8.5×10^{19}m^{-3} range (n_e/n_{GW}=0.3-0.8).

In this paper, we will report on the plasma radiation level during RF in section 2, on the plasma confinement in L modes and the access to H modes in section 3 and finally the current drive efficiency of LHCD will be presented.

2   PLASMA RADIATION DURING HIGH RF POWER INJECTION

The high radiation capability of high Z elements such as tungsten is a threat for maintaining a hot plasma with high energy confinement. Moreover, the neo-classical theory predicts an inward pinch of these impurities when the density and temperature profiles in the very core (r/a<0.3) are unfavorable. On WEST, since no NBI is used, the plasmas have a low toroidal rotation and are free of central particle source. Using GKW and NEO for the turbulent and neoclassical W transport respectively, we have found that the W neoclassical transport dominates over the turbulent one for r/a<0.25 [4]. Coherently tungsten accumulation is generally not an operational issue on WEST. Only in a few discharges, the tungsten asymmetry driven by ICRH could be the cause of an accumulation at low rotation [5].

Over the campaign C4 database of all pulses with at least 1MW of RF power, the fraction of the total power which is radiated in the bulk of the plasma Frad-Bulk is ranging from 30% to 50% for most of the discharges (figure1). On this large database, there is no strong effect of adding ICRH on top of LHCD (the mean Frad,bulk value increases from 47% to 49%). Low fraction of radiated power occurs after boronization of the torus. Frad-Bulk as low as 25% can be obtained with any combination of heating systems (LHCD, ICRH, LHCD+ICRH) as shown on figure 2. The reduction of Frad-bulk last 1-10 pulses depending on the energy injected. The mean Frad,bulk value around 50% is not modified with an increasing RF power. Frad-Bulk is also not density dependent at least up to n_e = 4.5×10^{19}m^{-3}. While for ohmic diverted plasmas this fraction is significantly higher: Frad-Bulk~65%, far from boronization, than the RF heated phase.
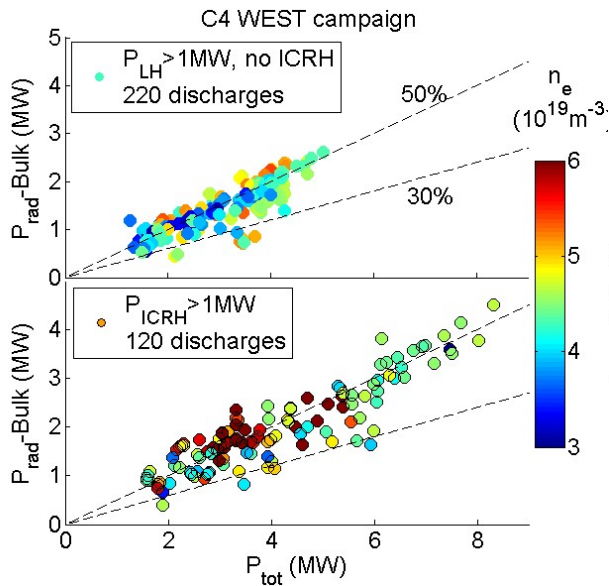

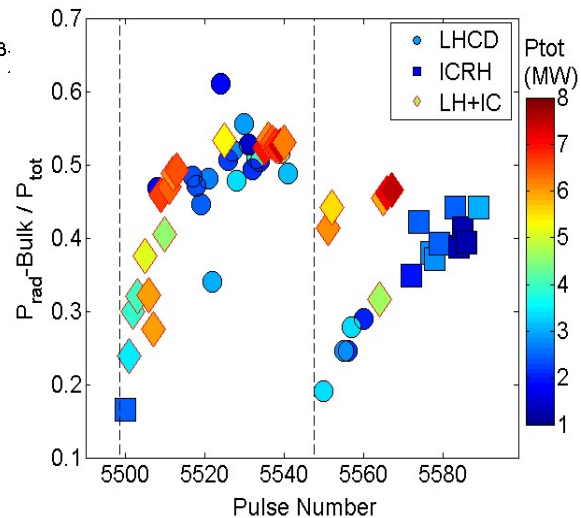Figure 1. Prad-Bulk as a function of total power (Bt=3.7T, Ip=0.5MA). The color-bar denotes the line-averaged density of the plasma

Figure 2. Time history of Frad-Bulk after two boronizations (dashed lines). The color-bar denotes the total power (Bt=3.7T, Ip=0.5MA).

Mid-Z species could be expected to contribute to the radiation of the bulk. On WEST, the main mid-Z species sputtered from the main chamber is copper. Modeling of a RF heated discharge (P_{LH}=4.6MW, Frad-Bulk=51%) with the 1½D code METIS [5] indicates that copper can be the main radiator at the plasma periphery (r/a>0.8) but does not contribute to the total bulk radiation by more than 20%.

In order to estimate the core W content, the 16 bolometry horizontal chords were inverted and, applying the cooling factors of tungsten to the local value of radiation, and accounting for the measured ECE T_e profile, a 6-point profile of tungsten density is obtained. The inversion is made up to T_e=1 keV, due to large uncertainties on the W cooling

factor below such temperatures [6]. The estimated n_W is divided by the electron density (inversion from 10 interferometry chords). The tungsten concentration in the core (r/a=0-0.22) is then plotted against the RF power. LHCD-only and ICRH- only pulses are compared in figure 3 a and 3b respectively. The W concentration in the core increases rather linearly with RF power and for a given power increases with Frad-bulk as long as the power does not exceed 3.5MW. At higher power, the core W radiation is more insensitive to Frad-Bulk. Similar trend was observed during the 2018 C3 campaign where the line-averaged electron density was mostly in the range of $3-4\times10^{19}m^{-3}$ while in C4 the density is above $4\times10^{19}m^{-3}$ [7].

Although the tungsten concentration can be rather large at high power, up to 4×10^{-4}, there is no correlation between this concentration and the energy confinement. It should be noted that the ohmic heating (OH) phase of these discharges have similar core W concentration (figure 3-a), but lower W density as the electron density is lower by a factor 1.6 on average. A similar trend, as for LHCD only pulses, is observed for ICRH discharges (figure 3-b) as long as no W accumulation occurs. High density discharges ($n_e>6.5\times10^{19}m^{-3}$) have low core tungsten concentration.
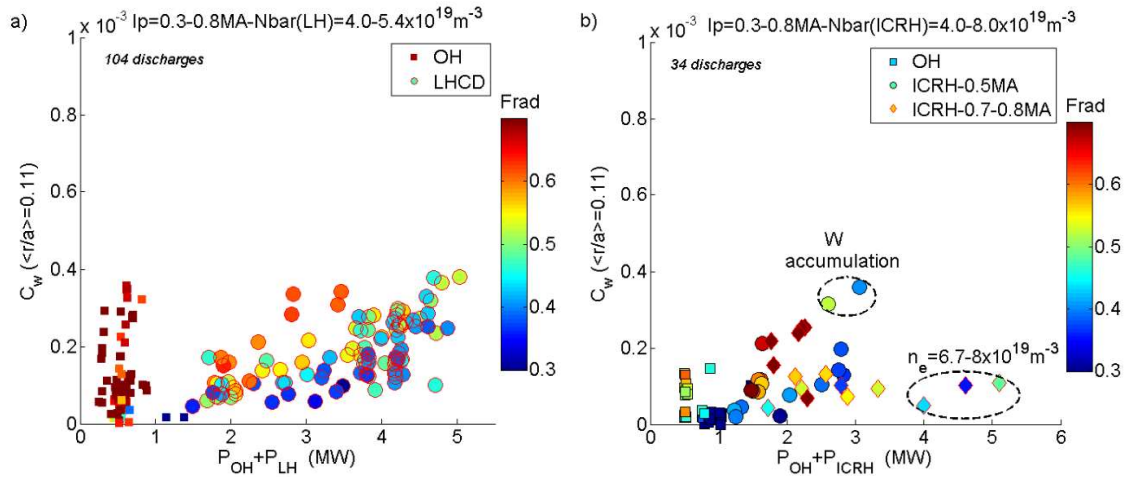

Figure 3. Core tungsten concentration of a) LHCD and b) ICRH (right) discharges. The concentration of the ohmic heating phase is also shown (squares). Data are averaged on one-second time slice.

During the early plasma current ramp up, tungsten central radiation often cools down the plasma in the center, leading to hollow electron temperature (T_e) profile and triggers MHD, likely 2/1 mode. Nitrogen injection during the current ramp-up induces an increase of the plasma resistivity in the peripheral region that leads to faster current diffusion, this increases the ohmic heating in the center and compensates for the plasma cooling due to W core radiation [8].
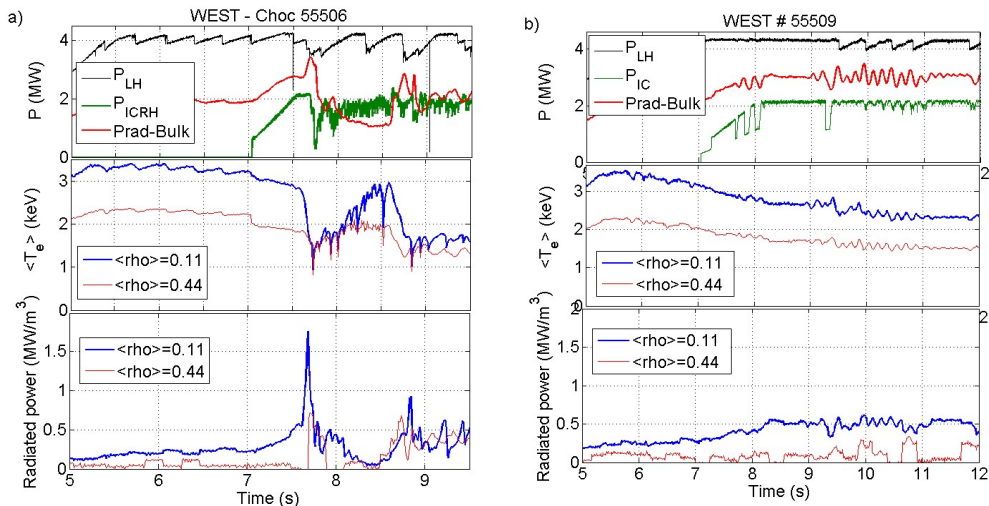

Figure 4. Two discharges a) with, b) without tungsten accumulation. Discharge 55506 has a wrong phasing of the ICRH straps between 7.0 and 7.65s.

Fast temperature collapse was observed when ICRH is added on top of LHCD with wrong phasing of the ICRH antenna strap (figure 4-a). With a proper dipole phasing (figure 4-b), tungsten density in the core increases proportionally to the total injected RF power (figure 4). It should be noted that accumulation starts at t~7.3s, 300ms before the strong increase of radiation and the temperature crash. When comparing the two discharges at the end of the ICRH power ramp (PICRH=2.1MW), the time when tungsten starts accumulating for discharge 55506, no difference in radiance of the W0 line (λ=407nm) for the 17 lines of sight viewing one of the two powered ICRH antenna is measured. Equilibrium and densities at the antennas are identical and therefore the tungsten sources (divertor and antenna) are unchanged, consistently with the total bulk radiation which does not increase for the wrong phasing case. To compare more precisely LHCD and ICRH only pulses with respect to the W radiation and content, two databases were built with matched average power (1.6 MW) and line-averaged density (4.8×10^{19}m^{-3}), one with LHCD only and the other with ICRH only. Frad-bulk increases on average from 47% (LHCD) to 54% (ICRH) with a standard deviation of 12-15%. The electron temperature is significantly lower for the ICRH discharges (-20% in the center) but the peaking is similar. For ICRH only pulses, the tungsten densities in the core (r/a<0.4) is higher by almost a factor 2 but with no sign of peaking (figure 5-a). Although the contribution of the tungsten in the core to the total radiation is small, it could be explain the lower electron temperature. Comparing LHCD-only and LHCD/ICRH discharges with same total power (3.7MW) and density (n_e=4.8×10^{19}m^{-3}), LHCD/ICRH discharges have a flatter temperature profile but a more peaked tungsten density profile in the core (r/a<0.4) (figure 5-b).
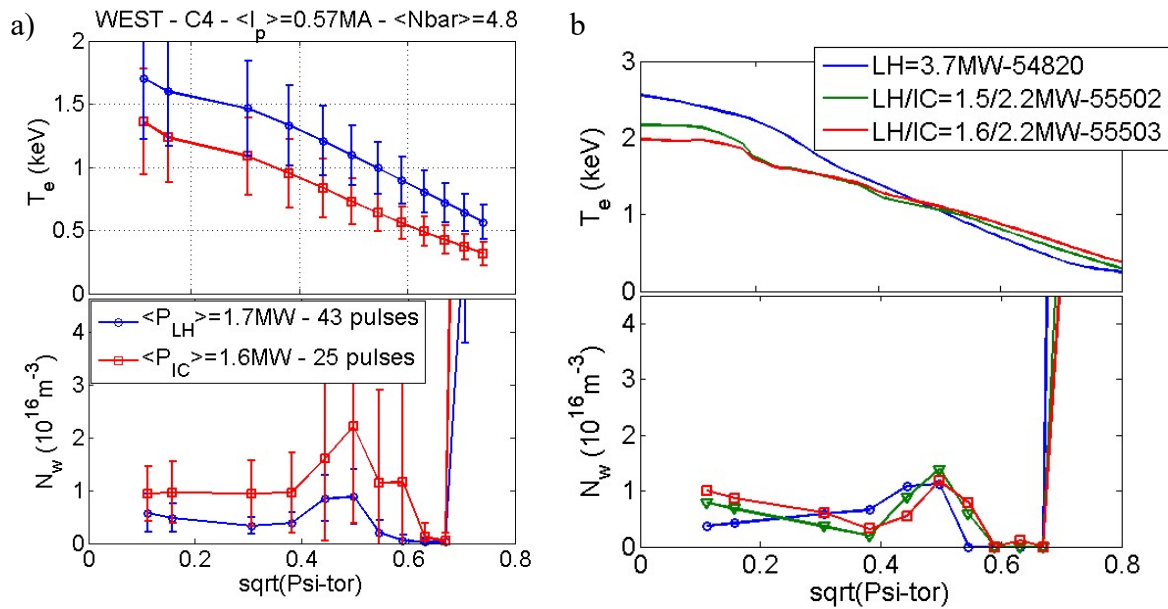

Figure 5. Electron temperature and tungsten profiles of a) LHCD and ICRH discharges, b) LHCD and LHCD/ICRH discharges with same total power. Tungsten densities at location where T_e is lower than 1keV are uncertain due to inaccurate knowledge of the cooling factor. Line averaged density n_e=4.8×10^{19}m^{-3}.

3.   ELECTRON HEATING AND ENERGY CONFINEMENT

Lower hybrid waves tailored for current drive (wave parallel index $N_{//}$=1.9 for these experiments) and ion cyclotron waves in the minority heating scheme (hydrogen minority concentration in the range of 5-10%) provide central electron heating after, respectively, slowing down of the fast electrons and collisional power redistribution of the fast ions. When the central electron temperature $T_e(0)$ is plotted as a function of the total power normalized to the volume-averaged density P_{tot}/n_{vol}, two regimes with different ranges of T_e0 are clearly seen (Figure 6). There is, first, a regime where the temperature increases with P_{tot}/n_{vol}. These discharges have high internal inductance and good global energy confinement whereas for the other discharges, the temperature does not increase beyond 2keV despite larger P_{tot}/n_{vol}. This reflects the difficulty of burning-through W, the W cooling factor increases for decreasing T_e leading to plasmas unstable with respect to any source of T_e reduction (increase of density for example). For a given W concentration, there is hence a threshold of centrally deposited electron heating necessary to allow for T_e to increase with P_{tot}/n_{vol}. For LHCD discharges for which the power deposition is rather large, this threshold is about 0.2MW/m^3 whereas ICRH

with more peaked power deposition, this threshold can be above $0.6MW/m^3$ with 3MW of RF power when pre-heated with LHCD.

Starting from the ohmic heating phase at low density ($n_e\sim2\times10^{19}$ m^{-3}, $T_e(0)$=1.5-2keV), the ramps of RF power and density need to be well adjusted in order to quickly cross this temperature window prone to temperature collapse, flattening of the current profile and triggering ultimately MHD activity. This is illustrated in figure 7: during a slow ramp of density, when the core radiation exceeds $0.15MW/m^3$, $T_e(0)$ decreases from 2.4keV to 1.7keV in 200ms and the MHD activity starts at this point.
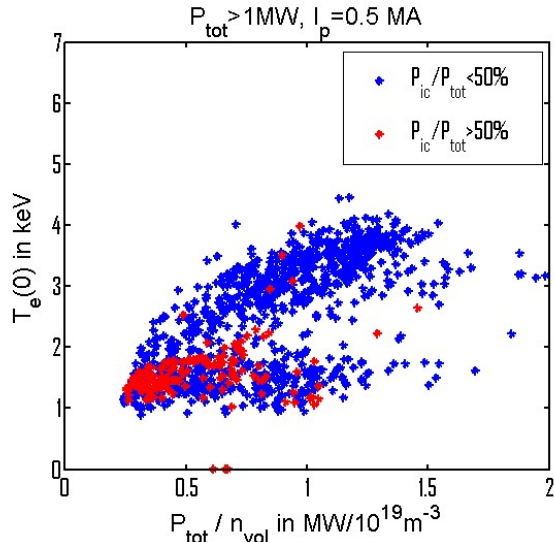
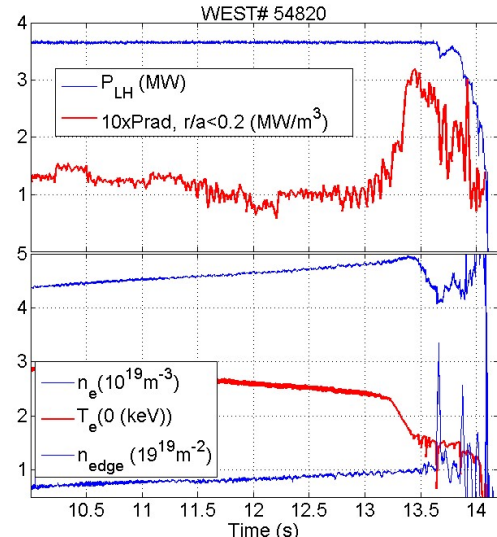Figure 6. Central electron temperature for LHCD and ICRH dominated discharges

Figure 7. Thermal instability of a LHCD discharge

Energy confinement is first evaluated with respect of the L-mode scaling law ITER-L-96P [9]. Interestingly, this scaling law was derived mostly for plasmas having an aspect ratio A ~3 and found almost no dependence with A. For LHCD discharges, the stored energy, W_{MHD}, increases according to this scaling law up to 300kJ (Figure 8). This confirms that the aspect ratio R/a (5.5-6 for these experiments) is not a scaling factor for the confinement. Confinement tends to be below the scaling when the density is increased indicating a weaker dependence on density in WEST than in the L-mode ITER scaling ($n_e^{0.4}$). From the WEST data (1313 entries), a new scaling leads to a $n_e^{-0.19}$ dependence but the scaling with power is similar. When the WEST database is merged with the ITER database (2400 entries), confinement scales as $n_e^{0.24}$ (Figure 9).
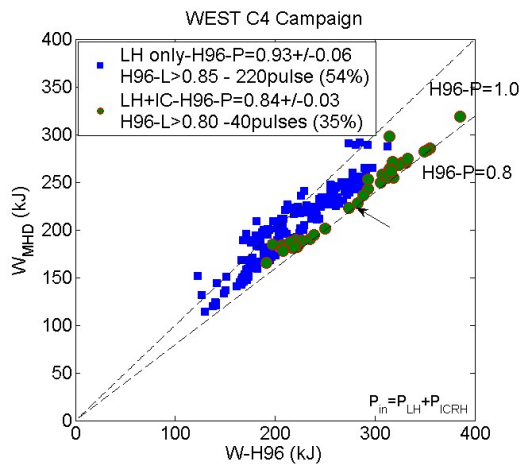
Figure 8. Stored energy of WEST discharges versus ITER-L-96P scaling law for LHCD only (squares) and LHCD+ICRH (circles) discharges.
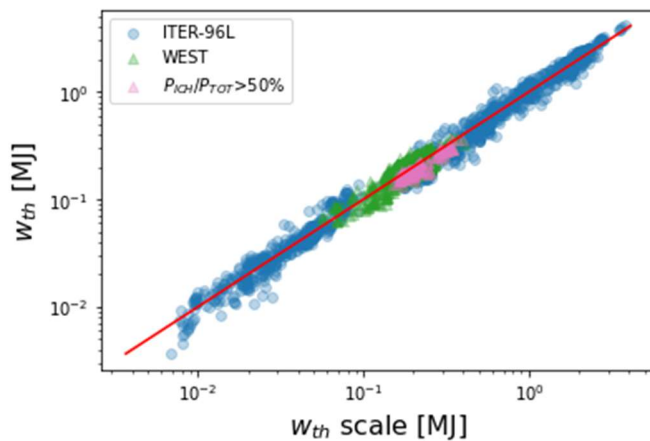
Figure 9. Stored energy of WEST and ITER databases versus a scaling law combining these two sets of data

Discharges combining LHCD with ICRH has lower energy confinement: averaged on a large number of discharges (Bt=3.7T, Ip=0.5MA) the H-factor is found to decrease from 0.93 (LHCD only) to 0.84 (LHCD+ICRH) (figure 8). The new scaling indicates the same trend. When ICRH is started on a discharge pre-heated with LHCD, very little central electron heating is generally observed, although the incremental bulk radiation can be as low as $\Delta P_{rad\text{-}Bulk}/P_{ICRH}$ ~35%. In the discharge shown in figure 10, comparing the LHCD phase (3MW) with the same LHCD+ICRH phase (2+3MW), the core plasma radiation (r/a<0.2) normalized to the total power and the fraction of radiated power Frad are reduced by 25%, but the central electron temperature and global confinement are lower in the combined heating phase. Large amplitude sawteeth indicate the presence of a fast ion population within the q=1 surface. These sawteeth do not cause a modulation of the core W density as observed at higher plasma current when the q=1 surface is larger. It should be noted that the LHCD+ICRH phase has a slighly more peaked T_e profile although density is slightly higher (~+10%) compared to the LHCD-only phase. Modeling of the LHCD and ICRH power depositions with METIS confirms more central, but also broader, power depostion for the phase combining the two RF heating systems (figure11). Inside the r/a=0.2 surface, the mean heating power increases by at least a factor two when the radiated power increases by less than 50% and would discard the effect of core radiation on lower electron heating than expected.
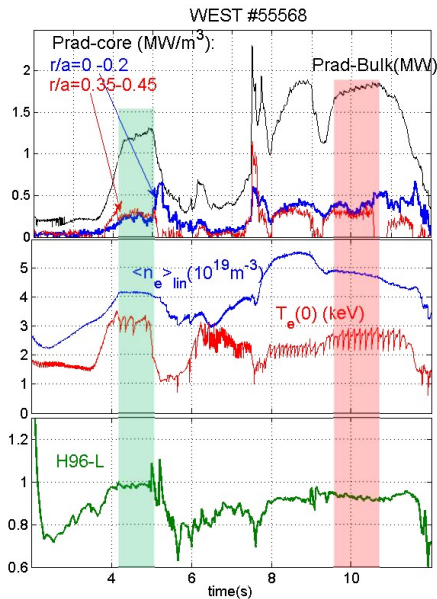
Figure 10. Discharge with a 3MW LHCD-only phase (green shaded) and a LHCD+ICRH phase (2MW+3MW, red shaded)
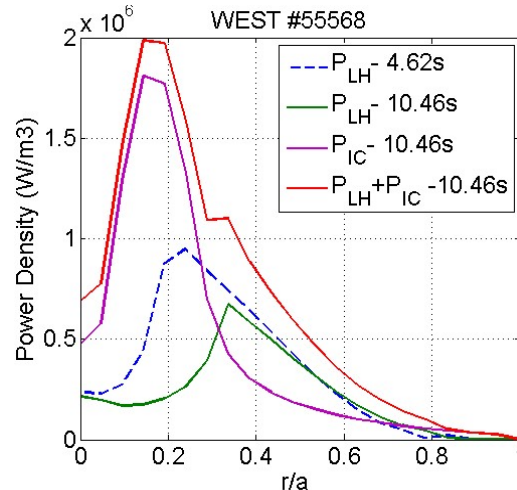
Figure 11. Power deposition of the discharge of figure 12 (METIS modeling)

L-H transition was observed, after fresh boronization, when combining 4MW of LHCD with 1MW of ICRH (Figure 12), both in LSN where the $\vec{B} \times \vec{\nabla} B$ is in the so-called favorable configuration as well as in the USN, so-called unfavorable configuration [10]. They occur for power crossing the separatrix slightly below the Martin 2008 scaling law and at densities below the minimum in density predicted by Ryter scaling [11], as illustrated in figure 13. Therefore, the ELM free transitions observed so far in WEST are likely transitions occurring on the low density branch. It results a significant increase of the particle confinement time (30% increase of plasma density with gas injection turned off) but, close to the L-H transition threshold, the stored energy increases by only 5-10%. The internal inductance decreases from 0.85 to 0.75 but the current driven by the LH waves does not flatten (the peaking of the HXR profile is unchanged), indicating a flattening of the total current profile caused by a higher bootstrap current at the edge. The radial electric field profile at the plasma edge, measured by Doppler back scattering, is more sheared (deeper well) after the transition [10].
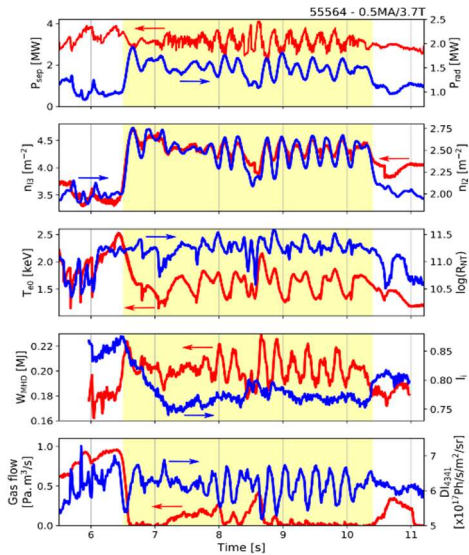
Figure 12. 4-second H-mode discharge in LSN configuration. Total power P_{tot} is the combination of 4MW of LHCD with 1MW of ICRH.
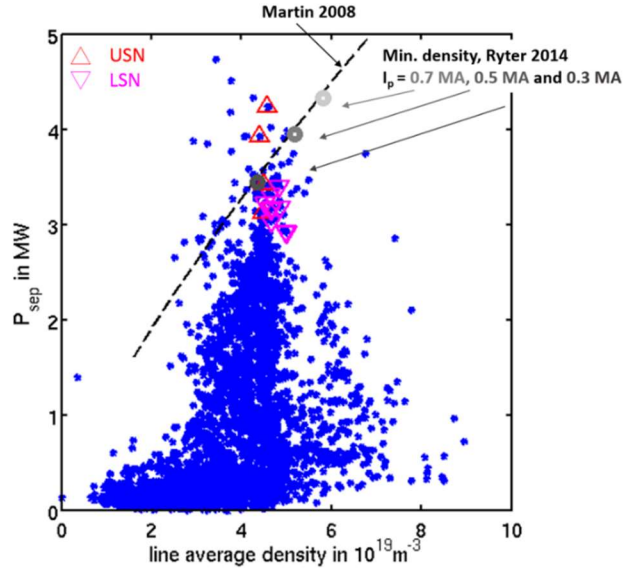

Figure 13. Psep versus density for the whole C4 campaign. The dashed line is the Martin's scaling for L-H transition (B=3.7T).

4. LOWER HYBRID CURRENT DRIVE

LHCD allows reducing the loop voltage down to ~0.1V up to $n_e=4 \times 10^{19} m^{-3}$ indicating a current drive efficiency of $0.7-0.8 \times 10^{19}$ A.W^{-1}m^{-2} when including the bootstrap current (I_{bs}/I_p=10-15%) (Figure 14). Higher efficiency (~0.8-0.9×10^{19} A.W^{-1}m^{-2}) was achieved after a fresh boronization or in upper single-null configuration. Remarkably, the discharge at the lowest density ($3 \times 10^{19} m^{-3}$) has a broader hard X-ray (HXR) emission profile than the higher density discharge (in upper single-null configuration) and a very similar LHCD efficiency. However the high density case has much higher bulk plasma radiation (far from boronization) and the screening from partially ionized tungsten atoms, although not affecting the LHCD efficiency, can increase strongly the bremsstrahlung. It results a decoupling between the LH current profile and the HXR profile [12].
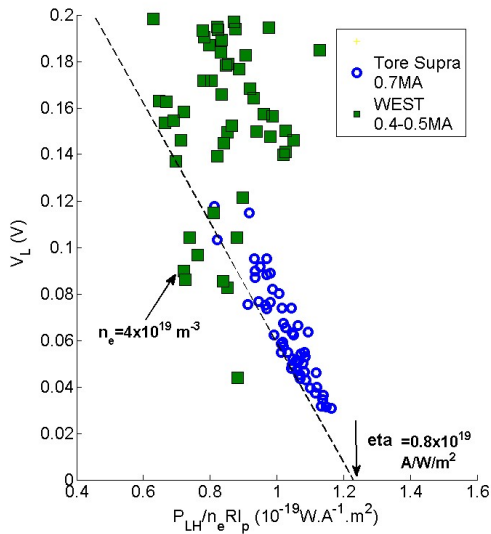

Figure 14. Loop voltage as a function of normalized LHCD power. All pulses below the dashed line with 50mV<V_L<110mV are in upper single-null configuration
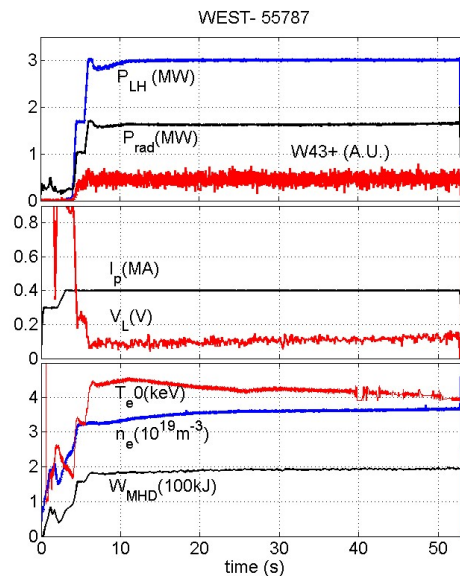

Figure 15. 53-second discharge (Bt/Ip=3.7T/0.4MA, USN configuration).

The polarization of the lower hybrid wave was inferred from a visible spectroscopy diagnostic measuring the D_β spectral line profiles, 3-6 centimeters in front of the launcher. At low density ($n_e < 4 \times 10^{19} m^{-3}$), the polarization is found to be as expected for the slow wave but at higher density, a significant rotation of the polarization is measured on some discharges, leading to a poloidal component which can be as high as the radial component. This can lead to a degraded current drive efficiency such as that observed on Alcator C-Mod [13].

A loop voltage of 130mV allows on WEST at medium density ($n_e = 3.7 \times 10^{19} m^{-3}$) extending the discharge duration to 53 seconds, although this duration was not limited by magnetic flux consumption (Figure 15). All plasma parameters are steady in particular the total radiation and the density of highly ionized tungsten atoms (W^{43+}) representative of the tungsten content in the core of the discharge as the variation of the electron temperature does not exceed 10%.

5. CONCLUSION

High RF power experiments combining LHCD and ICRH have been conducted on the full tungsten WEST tokamak up to 9MW. Without boronization the radiated power, due to W, is high (Frad,bulk~50%) but can be as low as 25% after boronization of the walls. Two types of pulses are obtained, some in which $T_e(0)$ increases with increasing P_{tot}/n_{vol} as expected, and some where the plasma does not burn-through W radiation and $T_e(0)$ remains below 2keV even with increasing P_{tot}/n_{vol}. However, on the hot branch, good performance L-mode plasmas with high electron temperature and high confinement (following the ITER L96 scaling) in stationary conditions are achieved despite Frad-bulk~50%. Thanks to more than additional 1000 entries in the ITER L mode database, the weak aspect ratio weak impact on the confinement is verified. For the access to H-mode this is still an issue as this improved confinement regime has been obtained so far only at a power exceeding marginally the threshold, and with oscillatory phases due to increasing radiation once the pedestal density forms. Although the ICRH antennas have been identified on other experiments as a main source of tungsten, when comparing LHCD discharges with ICRH or LHCD/ICRH discharges, the radiation is not significantly (see figure 1) higher in the latter case for most of the discharges. In WEST phase 2, the ICRH power will be further ramped up in order to maximize the central electron heating which should be favorable in particular to burn through tungsten. The H mode access will be explored at higher density and higher power. In order to perform very long pulses at high density ($>5 \times 10^{19} m^{-3}$) with 6MW of LHCD, an efficiency of 1×10^{19} A.W^{-1}m^{-2} is necessary to drive a current of 0.5MA. This should be possible with a larger bootstrap current.

REFERENCES

[1] BOURDELLE C. et al., Nucl. Fusion **55**, 063017 (2015)
[2] LIANG A.S. et al, optimization of LH wave coupling for the WEST LHCD launchers, this conference
[3] HILLAIRET J. et al, WEST actively cooled load resilient ICRH antenna results, this conference
[4] YANG, MANAS P. et al., Nucl. Fusion 60 (2020) 086012
[5] MAGET P. et al, Collisional transport and poloidal asymmetry distribution of impurities in tokamak plasmas, this conference
[6] ARTAUD J.F et al., Nucl. Fusion 58 (2018) 105001 (25pp)
[7] PÜTTERICH P.T. et al 2019 Nucl. Fusion 59 056013
[8] GONICHE M. et al., Plasma Phys. Control. Fusion 59 (2017) 055001
[9] BUCALOSSI J. et al., 'Operating a full tungsten actively cooled tokamak: overview of WEST first phase of operation', this conference.
[10] ITER Physics Basis, Nucl. Fusion 39 2175
[11] VERMARE L. et al., Formation of the radial electric field profile in WEST tokamak, this conference
[12] RYTER F., et al Nucl. Fusion **54** (2014) 083003
[13] PEYSSON Y.et al., Effect of partially ionized high-Z atoms on fast electron dynamics in tokamak plasma, this conference
[14] MARTIN E.H. et al., (2019), 59(7), 076006.